Coalescence of Deformable Granules in Wet Granulation Processes

L. X. Liu and J. D. Litster

Dept. of Chemical Engineering, University of Queensland, St. Lucia QLD 4072, Australia

S. M. Iveson

Centre for Multiphase Processes, Dept. of Chemical Engineering, University of Newcastle, Callaghan NSW 2308, Australia

B. J. Ennis

E. & G. Associates, 3603 Hoods Hill Road, Nashville, TN 37215

In this work, the coalescence of deformable granules in wet granulation processes is modelled. The model accounts for both the mechanical properties of the granules and the effect of the liquid layer at the granule surface. It is an extension to the model of Ennis et al. (1991) to include the possibility of granule plastic deformation during colli-sions. The model is written in dimensionless groups such as viscous and deformation Stokes numbers and the ratio of granule dynamic yield strength to granule Young's modulus (Y_d/E^*). These variables are bulk parameters of the powder-binder mixture and also functions of the process intensity. The model gives the conditions for two types of coalescence− type I and type II. Type I coalescence occurs when granules coalesce by viscous dissipation in the surface liquid layer before their surfaces touch. Type II coales-cence occurs when granules are slowed to a halt during rebound, after their surfaces have made contact. The model explains some of the trends observed in the literature, are preliminary validation of the coalescence criterion with drum granulation data is encouraging. An extension is also made to the case of surface dry granules, where liquid is squeezed to the surface during granule deformation.

Introduction

Wet granulation, a size-enlargement process, is a heavily used unit operation in a variety of industries (Ennis and Lit-ster, 1997), including pharmaceuticals, food, agricultural products, and metallurgical. It is an example of *particle de-sign* where the properties of the product granules are con-trolled by a combination of *process design* (varying process parameters in the granulator) and *formulation design* (adjust-ing the properties of the feed powders and liquid binder).

The evolution of granule properties during granulation is controlled by three classes of process: wetting and nucle-ation, growth and consolidation, and attrition and breakage (Ennis and Litster, 1997). In this article we consider only coa-lescence growth of granules. A very wide variety of granule growth behavior has been observed in the literature. Gener-ally speaking, these growth behaviors can be divided into two types: steady growth and induction time behavior (see Figure 1).

The type of growth depends on the deformability and rate of consolidation of the granules. For weak, deformable, and fast consolidating granules, a large contact area is formed during collision, and liquid binder will be easily squeezed into the contact zone, promoting steady growth. This is common in systems with coarse, narrow size distribution particles and low surface tension and/or low viscosity binder liquids (Ive-son and Litster, 1998a).

Strong, slowly consolidating granules do not deform suffi-ciently during impact to form a large area of contact, and liquid migration to the bond is also slow due to low consoli-dation. This subsequently leads to little or no growth—the "induction" period (also called the "nuclei" region (Kapur, 1978) or "compaction" period (Hoornaert et al., 1998)). How-
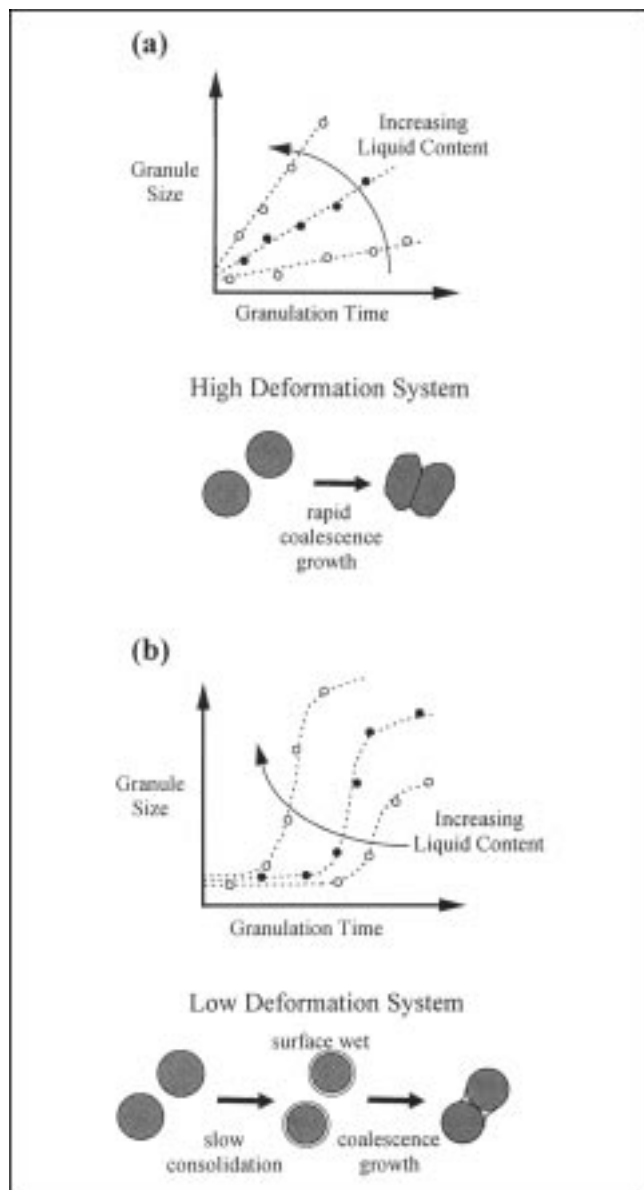
Figure 1. (a) Steady-Growth and (b) induction-growth behavior and controlling effect of granule deformability (by Iveson and Litster 1998a).

ever, when the granules are consolidated sufficiently, liquid binder may be squeezed to the granule surface enabling a liquid bond to form between colliding granules. The length of induction period decreases with increasing liquid content (Hoornaert et al., 1998). The induction time will become zero for liquid contents above a critical value giving rapid growth. This is because the granules formed from the initial nucleation stage are already fully saturated and covered by liquid binder. This class of behavior is frequent in systems with fine particles and/or viscous binders (Iveson and Litster, 1998a).

In a granulator, granules continually undergo impact collisions with neighboring granules. The granule growth behavior is fundamentally set by whether colliding granules stick together (coalesce) or rebound. This simple concept is diffi-

cult to model because of the complex nature of the granules. In the literature, there are a number of approaches to modeling granule coalescence. Ouchiyama and Tanaka (1975) considered surface-dry, deformable granules that collide without rebound. Successful coalescence was related to the strength of the bond formed. The separating force was assumed to be proportional to the granule volume. Kristensen et al. (1985) further extended the work of Ouchiyama and Tanaka by assuming that granule deformation for a given force was proportional to the ratio of critical strain and stress at failure measured during compression of bulk samples. Bond strength formed between granules was assumed to be the same as the bulk tensile strength of the granule.

A second approach is that of Ennis and coworkers (1991). They considered the collision of nondeformable, elastic granules with liquid layers at the surface. Successful coalescence depends on the viscous dissipation in the binder phase and losses in the granule (characterized by a coefficient of restitution) being sufficient to dissipate the energy of collision.

Other variations of this energy balance approach in the literature include considering elastic–adhesive collisions (Moseley and O'Brien, 1993) and elastic–plastic–adhesive collisions (Thornton and Ning, 1998) between particles. These models neglect the effects of liquid binder and assume only the presence of an adhesive energy that must be overcome for successful rebound.

Another approach is the rupture-energy method, which was developed by Simons and coworkers (1993). They proposed that the energy required to break the liquid bridge was proportional to the liquid-bridge volume. In this approach, only the static capillary force was considered.

None of these models is completely satisfactory. The Ouchiyama and Tanaka approach neglects the very important role of liquid at the granule surface. Ennis and coworkers neglected the role of plastic deformation at the contact point and do not consider nonsurface wet granules. Simons and coworkers ignore the effects of liquid viscosity and plastic deformation.

The aim of this study is to develop a more generalized coalescence criterion that accounts for the mechanical properties of the wet granules as well as the effect of liquid at the granule surface. We extend the model of Ennis et al. (1991) to include granule deformation behavior during collisions. The model is written in terms of measurable granule mechanical properties, liquid binder properties, and the characteristic collision velocity in the granulator. A sensitivity analysis of model parameters is given and results are compared with experimental studies of Iveson and Litster (1998a). The model is also extended to include the case of initially surface-dry granules where liquid binder is squeezed to the surface by the impact deformation.

Theory

A granule is a particle matrix partially or fully saturated with the binder liquid. We will assume the binder is an incompressible Newtonian liquid. We consider the granular matrix to be a simple elastic–plastic solid with stress–strain behavior shown by Johnson (1987). The granule mechanical behavior is characterized by an elastic modulus, E, and dynamic yield stress, Y_d. This mechanical properties are both

assumed to be strain-rate independent and not a function of stress–strain history.

If the granule is oversaturated with liquid, then it will have a liquid layer at the surface. Assuming that the liquid-layer thickness is much smaller than the granule diameter ($h_0 \ll D$), then the liquid layer thickness is

$$h_0 = \begin{cases} \dfrac{D(\nu - \epsilon s^*)}{6}; & \nu > \epsilon s^* \\ 0; & \nu < \epsilon s^*, \end{cases} \tag{1}$$

where D is the diameter of the granules (see Eq. 3b), ν is the volume fraction of liquid in the granule ($\nu = s\epsilon$), ϵ is the granule porosity, s is the granule saturation (ratio of liquid to pore volume), and s^* is the granule saturation at which a surface liquid layer first appears. Note that s^* should theoretically be unity, but may be less due to trapped air pockets inside the granules.

Now we derive a coalescence criterion for deformable, surface-wet granules, by extending the analysis of Ennis et al. (1991) using contact mechanics (Johnson, 1987) to account for elastic and plastic deformation of the granules during collision. Elastohydrodynamic collisions are of great interest in the fields of lubrication and filtration where many models have been developed to predict whether or not rebound will occur (such as Davis et al., 1986; Larsson and Höglund, 1994; Lian et al., 1996). These are, however, extremely complex events to model, usually requiring numerical solutions. Including the plastic properties of the solid phase will make an analytical solution impossible unless several major simplifications are made.

First, we will assume that the granule surfaces only begin to deform when they come into physical contact, whereas in reality the pressure generated by the fluid being squeezed between the surfaces will cause some precontact deformation. Second, it is assumed that interparticle attractive forces in the contact area are negligible. Third, it is assumed that fluid cavitation does not occur during granule rebound. We will also neglect the possibility of granule fracture and breakage, although for high strains this will become likely.

Another major simplification is that liquid capillary forces will be neglected. Capillary forces are not considered in the lubrication and filtration literature because the liquid phase is usually continuous. Ennis et al. (1991) justified neglecting capillary forces on the basis that the energy added during liquid-bridge formation and granule approach is canceled by the energy dissipated during granule separation and liquid-bridge rupture. However, even if the dynamic energies of pendular bridge formation and rupture are equal, they only cancel if the collision has a coefficient of restitution equal to one. Otherwise plastic and elastic losses in the granules will dissipate some of the capillary energy added during granule approach, meaning that there will be insufficient energy left to overcome the capillary forces during rebound. This effect may be significant in systems with low viscosity, high surface tension binders, but will not be considered in this current model. The dynamics of pendular liquid-bridge rupture are also extremely complex, but we will simply assume, as per Ennis et al. (1991), that the bridge ruptures at the distance at which it initially formed ($2h_0$).
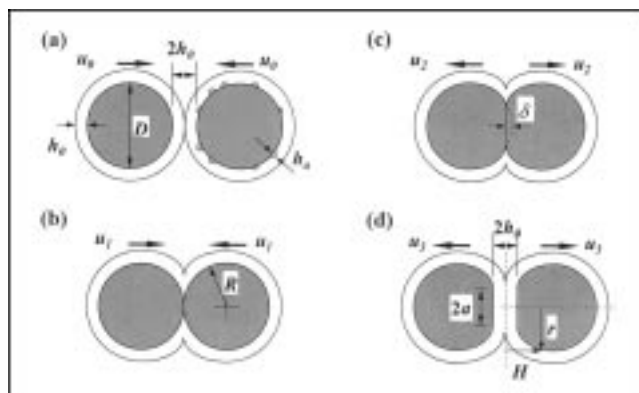

Figure 2. Model used to predict coalescence.
(a) Approach stage; (b) deformation stage; (c) initial separation stage, (d) final separation stage.

Consider a collision between two surface wet granules with a relative collision velocity $2u_0$ (see Figure 2). Assuming that the liquid-layer thickness is larger than the granule surface roughness, the collision can be divided into three stages:

1. *Approach stage.* At a separation distance of $2h_0$ the liquid layers touch and merge (Figure 2a). This combined liquid layer will then be squeezed out as the granules approach, dissipating some of the kinetic energy of collision.

2. *Deformation stage.* When the separation distance reduces to $2h_a$ (the height of granule surface asperities) and the relative granule velocity to $2u_1$ (Figure 2b), the granules will begin to deform. The remaining kinetic energy is converted to stored elastic energy and dissipated by plastic deformation. When the relative collision velocity is reduced to zero, a contact area A^* is formed between the granules.

3. *Separation stage.* The granules then begin to rebound with an initial velocity of u_2 as the stored elastic energy is released (Figure 2c). Viscous dissipation in the surface liquid layer will again retard the granule movement. When the granules are separated to a distance $2h_0$, the liquid layers are assumed to separate and the granule rebound is complete, leaving the granules with a velocity of u_3 (Figure 2d).

The granules will coalesce if the collision kinetic energy is completely dissipated by viscous losses in the surface liquid layer and plastic deformation in the granule matrix, that is, the granule collision velocity reduces to zero in either the initial approach stage (type I coalescence) or the final separation stage (type II coalescence). Granules will rebound (no coalescence) if there is some remaining granule velocity at the end of the separation stage ($u_3 > 0$).

We now look at each stage in turn. Ignoring the effect of capillary forces and assuming creep flow between two spheres, the equation of motion for the approach stage is (Ennis et al., 1991):

$$-\tilde{m}\frac{du}{dt} = \frac{3}{4}\pi\mu\tilde{D}^2\frac{u}{2h}, \tag{2}$$

where $\tilde{m}$ and $\tilde{D}$ are the harmonic mean granule mass and

diameter for two unequal sized granules given by

$$\tilde{m} = \frac{m_1 m_2}{m_1 + m_2} \tag{3a}$$

$$\tilde{D} = \frac{D_1 D_2}{D_1 + D_2} \tag{3b}$$

and $2h$ is the separation distance between the granule surfaces Integrating Eq. 3, the collision velocity when the granules reach a separation distance of $2h_a$ and start to deform, is

$$u_1 = u_0 \left[1 - \frac{1}{St_\nu} \ln\left(\frac{h_0}{h_a} \right) \right], \tag{4}$$

where St_ν is the viscous Stokes number given by

$$St_\nu = \frac{8\tilde{m} u_0}{3\pi \mu \tilde{D}^2}. \tag{5}$$

If the viscous force is so high that the granule velocity u_1 is less than zero, then coalescence will occur before the granule surfaces come into contact. We define this type of coalescence as *type I coalescence*, and the conditions can be written as follows:

$$St_\nu < \ln\left(\frac{h_0}{h_a} \right). \tag{6}$$

The main characteristic of type I coalescence is that granules are halted and coalesce before their surfaces come into contact.

For granules with $u_1 > 0$, at the separation distance of $2h_a$, the granule surfaces come into contact and begin to deform. The pressure at the initial contact point is high and yield is initiated at a point beneath the surface. Up to the instant of maximum compression, the kinetic energy absorbed in local deformation of the two granules is

$$\frac{1}{2}\tilde{m}(2u_1)^2 = \int_0^{\delta^*} pA \, d\delta, \tag{7}$$

where δ is the average compression distance and δ^* is the maximum compression, p is the mean contact pressure during impact, and A is the contact area. Although the material in the impact zone wants to start flowing at its unconfined yield stress, Y_d, surrounding material prevents it. Johnson (1987) showed experimentally that the mean contact pressure can be approximated by $3.0 Y_d$. For $\delta \ll \tilde{D}$, the compression is related to the contact area by

$$A = \pi\tilde{D}\delta, \tag{8}$$

that is, assuming neither ''piling up'' nor ''sinking in'' occurs at the edge of the indentation (Johnson, 1987). Substituting Eq. 8 into Eq. 7 and integrating, gives

$$2\tilde{m} u_1^2 = \frac{3 A^{*2} Y_d}{2\pi\tilde{D}}. \tag{9}$$

Rearranging Eq. 9, we have the maximum deformation area:

$$A^* = \pi\tilde{D}\delta^* = 2u_1 \left[\frac{\pi\tilde{m}\tilde{D}}{3Y_d} \right]^{1/2}. \tag{10}$$

At this maximum compression, granules start to rebound with the stored elastic energy. The stored elastic energy, E_e, is given by (Johnson, 1987):

$$E_e = \frac{3}{10} \frac{\pi^2 a^{*3}(3Y_d)^2}{E^*}, \tag{11}$$

where a^* is the radius of the maximum deformed area ($A^* = \pi a^{*2}$) and E^* is given by

$$\frac{1}{E^*} = \frac{1 - \nu_1^2}{E_1} + \frac{1 - \nu_2^2}{E_2}, \tag{12}$$

where E_1 and E_2 are Young's modulus of the two granules and ν_1 and ν_2 are the Poisson ratios, respectively. Substituting a^* from Eq. 10 into Eq. 11 yields

$$E_e = \frac{3}{10} \frac{(3\pi Y_d)^{5/4}(\tilde{m}\tilde{D})^{3/4}(2u_1)^{3/2}}{E^*}. \tag{13}$$

Taking the rebound to be elastic, the stored elastic energy is converted into an initial rebound velocity u_2:

$$\frac{1}{2}\tilde{m}(2u_2)^2 = E_e. \tag{14}$$

Combining Eqs. 13 and 14, we have the initial rebound velocity of each granule u_2:

$$u_2 \approx 2.46 \left(\frac{Y_d}{E^*} \right)^{1/2} \left(\frac{\tilde{m} u_1^2}{2\tilde{D}^3 Y_d} \right)^{-1/8} u_1. \tag{15}$$

Substituting for u_1 from Eq. 4 into Eq. 15 yields

$$u_2 \approx 2.46 u_0 \left(\frac{Y_d}{E^*} \right)^{1/2} \left(\frac{\tilde{m} u_0^2}{2\tilde{D}^3 Y_d} \right)^{-1/8} \left(1 - \frac{1}{St_\nu} \ln\frac{h_0}{h_a} \right)^{3/4}. \tag{16}$$

Now consider the separation stage. Initially, the geometry during the separation phase consists of two flat surfaces of radius a^*, plus the remains of the spherical surfaces (Figure 2c and 2d). As the elastic energy is released to accelerate the granules to velocity u_2, however, the deformed area will reduce due to some elastic recovery. The extent of elastic recovery, δ', is given by (Johnson, 1987):

$$\delta' = \frac{9\pi a^* Y_d}{4E^*} = \frac{9\pi Y_d}{4E^*} \left(\frac{2u_1}{\pi} \right)^{1/2} \left(\frac{\pi\tilde{m}\tilde{D}}{3Y_d} \right)^{1/4}. \tag{17}$$

Hence the permanent plastic deformation, δ'' is

$$\delta'' = \delta^* - \delta' = \left(\frac{8}{3\pi}\right)^{1/2} (St_{\text{def}})^{1/2} \tilde{D}\left[1 - \frac{1}{St_\nu}\ln\left(\frac{h_0}{h_a}\right)\right]$$

$$\times \left\{1 - 7.36\left(\frac{Y_d}{E^*}\right)(St_{\text{def}})^{-1/4}\left[1 - \frac{1}{St_\nu}\ln\left(\frac{h_0}{h_a}\right)\right]^{-1/2}\right\}, \quad (18)$$

where

$$St_{\text{def}} = \frac{\tilde{m}u_0^2}{2\,\tilde{D}^3 Y_d} \quad (19)$$

is the Stokes deformation number for the collision (Tardos et al., 1997; Iveson and Litster, 1998a), which gives a measure of the amount of plastic deformation that the granule would have suffered during the collision had there been no viscous liquid layer present. Please note that because of the simplification that $p = 3.0\ Y_d$ used to derive δ^*, for small amounts of deformation (low u_1) it is possible for Eq. 18 to predict a negative value of δ'' (which is a physical impossibility). When this occurs, assume that $\delta'' = 0$ and $e = 1$.

The viscous force for squeeze flow of a Newtonian liquid between two axisymmetric particles is given by (Adams and Edmondson, 1987)

$$F_{\text{vis}} = \frac{3\pi\mu}{2}\frac{dh}{dt}\int_0^R \frac{r^3}{[H(r)]^3}\,dr, \quad (20)$$

where $H(r)$ is the half distance between the two surfaces at a radial distance r from the axis of symmetry (Figure 2d). An analytical solution to this integral is possible for $h \ll \tilde{D}$ by using the approximations $H(r) \approx h - \delta'' + r^2/2R$ (for $r > a$), $H(r) = h$ (for $r < a$), and $(a)^2 \approx \delta\tilde{D}$ to obtain:

$$F_{\text{vis}} = \frac{3\pi\mu\tilde{D}^2}{8}\left(\frac{(\delta'')^2}{h^3} + \frac{\delta''}{h^2} + \frac{1}{h}\right)\frac{dh}{dt}. \quad (21)$$

For negligible deformation ($\delta'' \approx 0$) this reduces to

$$F_{\text{vis}} = \frac{3\pi\mu R^2}{2h}\left(\frac{dh}{dt}\right), \quad (22)$$

which is the equation for squeeze flow between two spheres used in the original model of Ennis et al. (1991). In this case, the model will give the same critical viscous Stokes number (St_ν^*) for coalescence:

$$St_\nu^* = \left(1 + \frac{1}{e}\right)\ln\left(\frac{h_0}{h_a}\right), \quad (23)$$

except that the coefficient of restitution (e) is not a constant, but varies with the velocity of impact according to the equation (Johnson, 1987):

$$e = \frac{u_2}{u_1} = 2.46\left(\frac{Y_d}{E^*}\right)^{1/2}\left[1 - \frac{1}{St_\nu}\ln\left(\frac{h_0}{h_a}\right)\right]^{-1/4}(St_{\text{def}})^{-1/8}. \quad (24)$$

For large deformations ($\delta'' \gg h$), Eq. 21 reduces to

$$F_{\text{vis}} = \frac{3\pi\mu(a)^4}{8h^3}\left(\frac{dh}{dt}\right), \quad (25)$$

which is the equation for squeeze flow between two flat plates.

The full equation for the movement of the two flattened spheres during rebound is

$$-\tilde{m}\frac{du}{dt} = \frac{3\pi\mu\tilde{D}^2}{8}\left(\frac{(\delta'')^2}{h^3} + \frac{\delta''}{h^2} + \frac{1}{h}\right)\frac{dh}{dt}. \quad (26)$$

Integrating Eq. 26, the granule velocity u_3 at a separation distance of $2h_0$ (where it is assumed the bridge will rupture) is

$$u_3 = u_2 - \frac{3\pi\mu\tilde{D}^2(\delta'')^2}{16\tilde{m}h_0^2}\left[\left(\frac{h_0^2}{h_a^2} - 1\right)\right.$$

$$\left. + \frac{2h_0}{\delta''}\left(\frac{h_0}{h_a} - 1\right) + \frac{2h_0^2}{(\delta'')^2}\ln\left(\frac{h_0}{h_a}\right)\right]. \quad (27)$$

Substituting for $(\delta'')^2$ from Eq. 18 into Eq. 27 yields

$$u_3 = u_2 - \frac{\mu u_1^2 \tilde{D}}{4Y_d h_0^2}\left[\left(\frac{h_0^2}{h_a^2} - 1\right) + \frac{2h_0}{\delta''}\left(\frac{h_0}{h_a} - 1\right)\right.$$

$$\left. + \frac{2h_0^2}{(\delta'')^2}\ln\left(\frac{h_0}{h_a}\right)\right]\left\{1 - 7.36\left(\frac{Y_d}{E^*}\right)(St_{\text{def}})^{-1/4}\right.$$

$$\left. \times\left[1 - \frac{1}{St_\nu}\ln\left(\frac{h_0}{h_a}\right)\right]^{-1/2}\right\}^2. \quad (28)$$

For granules to coalesce, u_3 must be less than or equal to zero. By setting $u_3 < 0$ and substituting for u_2 from Eq. 16 and u_1 from Eq. 4 into Eq. 28, we have the condition for type II coalescence:

$$\left(\frac{Y_d}{E^*}\right)^{1/2}(St_{\text{def}})^{-9/8} < \frac{0.172}{St_\nu}\left(\frac{\tilde{D}}{h_0}\right)^2\left[1 - \frac{1}{St_\nu}\ln\left(\frac{h_0}{h_a}\right)\right]^{5/4}$$

$$\left[\left(\frac{h_0^2}{h_a^2} - 1\right) + \frac{2h_0}{\delta''}\left(\frac{ho}{h_a} - 1\right) + \frac{2h_0^2}{(\delta'')^2}\ln\left(\frac{h_0}{h_a}\right)\right]$$

$$\left\{1 - 7.36\left(\frac{Y_d}{E^*}\right)(St_{\text{def}})^{-1/4}\left[1 - \frac{1}{St_\nu}\ln\left(\frac{h_0}{h_a}\right)\right]^{-1/2}\right\}^2. \quad (29)$$

The ratio δ''/h_0 can be found using Eq. 18.

If the elastic recovery term is ignored (that is, use δ^* rather than δ''), then the following simpler solution is obtained:

$$\left(\frac{Y_d}{E^*}\right)^{1/2}(St_{\text{def}})^{-9/8} < \frac{0.172}{St_\nu}\left(\frac{\tilde{D}}{h_0}\right)^2\left[1 - \frac{1}{St_\nu}\ln\left(\frac{h_0}{h_a}\right)\right]^{5/4}$$

$$\left[\left(\frac{h_0^2}{h_a^2} - 1\right) + \frac{2h_0}{\delta}\left(\frac{h_0}{h_a} - 1\right) + \frac{2h_0^2}{\delta^2}\ln\left(\frac{h_0}{h_a}\right)\right]. \quad (30)$$

Furthermore, if only the viscous force between the two flat surfaces is considered (Eq. 25), the condition for type II coalescence becomes:

$$\left(\frac{Y_d}{E^*}\right)^{1/2}(St_{\text{def}})^{-9/8} < \frac{0.172}{St_\nu}\left(\frac{\tilde{D}}{h_0}\right)^2\left[1 - \frac{1}{St_\nu}\ln\left(\frac{h_0}{h_a}\right)\right]^{5/4}$$
$$\left(\frac{h_0^2}{h_a^2} - 1\right). \quad (31)$$

The main characteristics of type II coalescence is that granules are slowed to a halt during rebound, after their surfaces have contacted. Whether or not permanent plastic deformation has occurred depends on the elastic–plastic properties of the granule (that is, if e from Eq. 24 is less than one, then some plastic deformation will have occurred).

The liquid layer thickness h_0 can be written in terms of the granule size and relative saturation (Eq. 1). If the height of asperities on the granule surface h_a is assumed to be proportional to the diameter of the constituent particles making up the granule (that is, $h_a = kD_p$, where k is less than or equal to $1/2$, we have the following equations for the dimensionless groups:

$$\frac{\tilde{D}}{h_0} = \frac{6}{\nu - \epsilon s^*} \quad (32)$$

$$\frac{h_0}{h_a} = \frac{\nu - \epsilon s^*}{6k}\frac{\tilde{D}}{D_p}. \quad (33)$$

Substituting Eqs. 32 and 33 into Eq. 29 yields the condition for type II coalescence in terms of granule excess liquid and the diameters of the constituent particles. Similarly, the condition for type I coalescence (Eq. 6) can be rewritten as

$$St_\nu < \ln\left(\frac{\nu - \epsilon s^*}{6k}\frac{\tilde{D}}{D_p}\right). \quad (34)$$

Equations 6 and 29 give us the conditions for type I and II coalescence of deformable, surface-wet granules in terms of measurable formulation properties and the characteristic collision velocity in the granulator.

Discussion

Equations 6, 29 and 34 show that granule coalescence depends on the following dimensionless parameters:
• The viscous Stokes number St_ν, which is the ratio of impact kinetic energy to viscous dissipation in the liquid layer
• The Stokes deformation number St_{def}, which is the ratio of impact kinetic energy to plastic deformation in the granule matrix
• The ratio of plastic yield stress to elastic modulus, Y_d/E^*
• The ratio of liquid-layer thickness to surface asperity height h_0/h_a (or its equivalent the excess liquid content $\nu - \epsilon s^*$), which gives the amount of liquid at the granule surface to aid coalescence
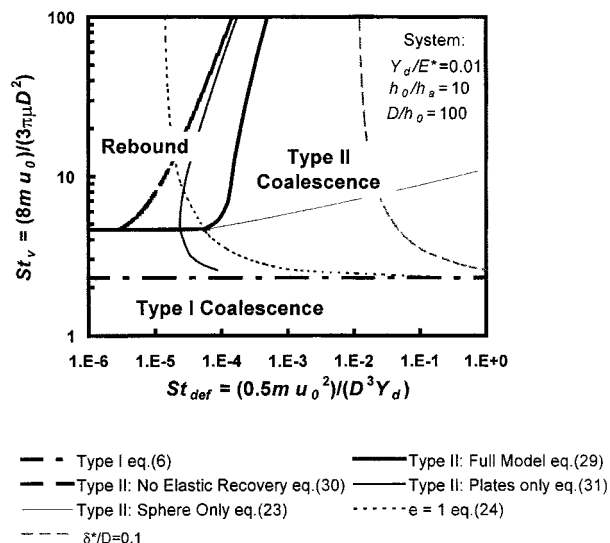

Figure 3. St_ν vs. St_{def} showing the boundaries for types I and II coalescence.

• The ratio of granule size to liquid layer thickness D/h_0 (or the related term $\tilde{D}/D_p$), which influences the relative importance of liquid layer to inertial effects.

Figure 3 is a plot of St_ν vs. St_{def} showing the two coalescence criteria (Eqs. 6 and 29) for two granules for given values of Y_d/E^*, h_0/h_a, and $\tilde{D}/h_0$. This plot shows the complex nature of the granule impact. Equations 6 and 29 divide the plot into three regions: type I coalescence, type II coalescence, and rebound. For type I coalescence, granules are stopped by viscous dissipation in the surface liquid layer before the granule surfaces touch. This occurs for all collisions below a critical value of St_ν, independent of St_{def} since the mechanical properties of the granule do not come into play. Therefore, Eq. 6 is a horizontal line in Figure 3.

For type II coalescence (Eq. 29) the relationship is more complex. For weak, deformable granules (high St_{def}), type II coalescence may occur even at quite high St_ν. There are two reasons for this:

1. A significant proportion of the impact kinetic energy is absorbed in plastic deformation of the granule matrix. Note that Eq. 24 shows that the granule coefficient of restitution is not a fundamental granule property, but decreases with increasing velocity of impact (Johnson, 1987).

2. The viscous dissipation during the separation stage (Eq. 21) is strongly related to the contact area generated by plastic deformation [$F_{\text{vis}} \propto (\delta''\tilde{D})^2 = (a^*)^4$ or A^2].

Hence, as more deformation occurs, the viscous forces during separation increase much more rapidly than the amount of stored elastic energy. As granule strength increases (decreasing St_{def}), the critical St_ν for type II coalescence approaches a minimum value given by the original model of Ennis et al. (1991) for zero plastic deformation.

All collisions to the left of the line showing coefficient of restitution (e) equal to 1 are perfectly elastic in nature with no permanent deformation of the granules. In this region, the model of Ennis et al. (1991) is valid. The current model
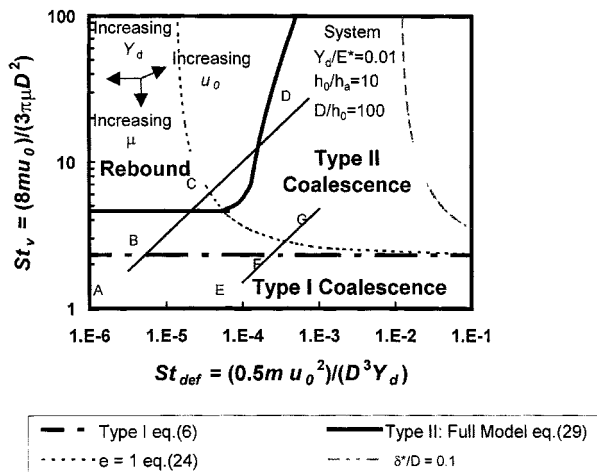
Figure 4. Effect of increasing initial impact velocity, yield stress, and liquid viscosity on coalescence behavior.

meets up with the predictions of Ennis's simpler model at the point where the $e = 1$ line intersects.

Figure 3 also shows the line where the ratio $\delta^*/\tilde{D}$ is equal to 0.1. The current model is only valid in the region to the left of the $\delta^*/D = 0.1$ line. This is because Eq. 8 and Eq. 18 assume that $\delta^* \ll \tilde{D}$. In addition, granule fracture and breakage are likely to occur at high strains, but this effect has been neglected in the present analysis. Hence, results to the right of this line should be treated with caution.

Also shown on Figure 3 are the predictions of the more simplified models. Equation 30 neglected the elastic recovery of the deformed area, and hence overpredicts the viscous force during rebound, thus increasing the likelihood of coalescence. Equation 31 only considers the viscous forces due to the flattened surfaces of the granules. Hence, it incorrectly predicts that the likelihood of coalescence decreases as St_v approaches the type I coalescence boundary, since if no deformation takes place, there is no flattened surface to create a viscous force during rebound. Equation 23 considers the rebounding granules as spheres only, and hence underestimates the viscous force on rebound for all cases where permanent deformation takes place.

In summary, then, the three regions are: *rebound* (strong granules at large St_v); *type I coalescence* (small St_v independent of granules strength); and *type II coalescence* (weak granules at a wide range of St_v).

Sensitivity to formulation properties and process parameters

Process Parameters. The key process parameter is the effective collision velocity u_0 that characterizes the process intensity. As u_0 increases, St_{def} and St_v will both increase, moving a system's behavior toward the top right of the plot. Figure 4 shows two cases of increasing impact velocity. For both weak and strong granules, at low impact velocities, the granule velocity is reduced to zero by the viscous force in the binder so type I coalescence occurs (points A and E). As u_0 increases further, the viscous force of the binder is not suffi-

cient to reduce the granule velocity to zero at surface contact (u_1), but u_0 is also not high enough to cause permanent deformation on the granules. The granule velocity at separation u_3 is reduced to zero before complete rebound occurs. Thus type II coalescence with no permanent deformation occurs (points B, F). As collision velocity increases further, the behavior depends on the strength of the granules. For weak granules (low Y_d), a large area of contact is formed, which generates large viscous forces during separation, preventing complete rebound (point G), Hence type II coalescence still occurs. For strong granules (high Y_d), the deformation area only increases slowly with impact velocity (Eq. 10), and so there is insufficient viscous force during rebound to prevent separation; hence, rebound occurs (point C). As the impact velocity increases further (increasing St_{def}), however, eventually a large area of contact is formed that generates a large enough viscous force to prevent rebound and type II coalescence occurs again (point D).

Hence, this model predicts that deformable systems that do not coalesce at low velocities may coalesce at higher velocities. This prediction is the opposite of that from the model of Ennis et al. (1991), which predicts that increasing impact speed always decreases the likelihood of coalescence. There is some tentative experimental evidence to support these new predictions. In a high shear mixer (where the high impact forces cause significant amounts of deformation), Schaefer et al. (1990) found that increasing impeller speed increased the initial rate of granule growth, which is opposite to the predictions of Ennis et al., but in full agreement with the current model. However, this increase in growth rate may be due solely to the increased frequency of collisions, so further work is required to confirm these predictions. In addition, breakage will always become an important issue as impact speed increases.

Formation Parameters. The granulation literature clearly identifies liquid content as having a major effect on granule growth. Figure 5 will show how the coalescence/rebound boundaries for both type I and type II coalescence change with changes to the excess liquid. As expected, increasing liquid content increases the critical Stokes number for both type I and type II coalescence, due to the increased binder-layer
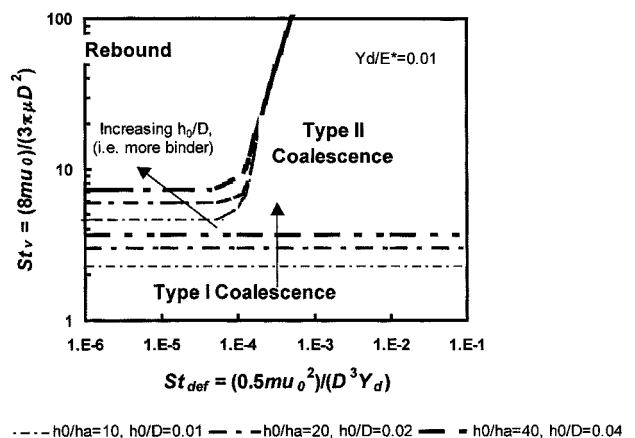

Figure 5. Effect of binder content on the coalescence criteria.

thickness, and hence increased viscous dissipation in the binder. However, as St_{def} increases, the effect of liquid content on the type II boundary becomes less significant, since for large contact areas, the viscous force during separation is much more sensitive to the size of contact area than the binder layer thickness (Eq. 18 and Eq. 23).

Increasing binder viscosity will shift a system down the plot (Figure 4), as St_v is inversely proportional to binder viscosity (μ); this should increase the probability of type I and type II coalescence. However, increasing μ also increases the dynamic yield strength of granules (Iveson and Litster, 1998b). Hence, increasing μ will decrease St_{def}, shifting a system's behavior toward the left, which might decrease the likelihood of type II coalescence (Figure 4). However, provided the decrease in St_{def} is not as great as the decrease in St_v (and assuming that Yd/E^* does not change), then increasing binder viscosity should always increase the likelihood of coalescence.

Increasing granule dynamic strength (such as by decreasing particle size) decreases St_{def}, which will shift a system's behavior toward the left of the graph. Provided that the increase of dynamic strength does not change other properties of the system (such as Y_d/E^*), this may decrease the probability of type II coalescence for large St_v. However, for St_v below the critical value predicted in Eq. 23, the dynamic yield strength has no effect on the coalescence conditions.

Other variables such as particle roughness, shape, and size distribution are not considered directly in this model. However, the effects of these variables should be implicitly accounted for by their effect on the granule mechanical properties (E^* and Y_d). Since it is extremely difficult to isolate the effect of these variables on granulation behavior, it is currently impossible to verify this assertion.

The greatest weakness of this model is the highly idealized, two-parameter mechanical model of the granule. The assumption that Y_d and E^* are strain-rate independent is unlikely to be true, particularly for granules bound by viscous binders at high strain rates. Even at low strain rates, the flow stress of water-bound, submicron alumina particle compacts has been observed to increase with strain rate (Franks and Lange, 1999). This highlights the importance of measuring the mechanical properties of granular material at strain rates that are comparable to those experienced in the granulation application being studied.

Only two other factors have been neglected in this model. One is the effect of capillary forces, and the second is the possibility of interparticle bonding when the granule surfaces deform against each other. Both these effects will increase the likelihood of coalescence and will be studied in future research.

Extension to surface-dry granules

It is implicit in this analysis that granules with any degree of elasticity will only coalesce if there is a liquid layer between them. This occurs automatically if the granules begin with a surface layer of liquid binder. In many applications, however, granules also coalesce if liquid binder becomes available in the bond zone to help hold them together. The exact mechanism of liquid transport into the bond zone is unclear, since most granular materials dilate during strain, which would tend to suck liquid away from the contact zone.
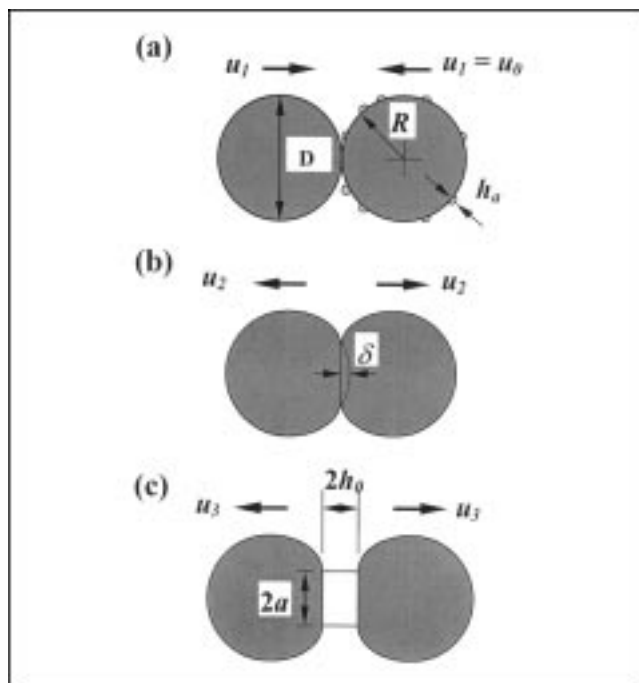

Figure 6. Model for collision of surface dry granules.

Perhaps this liquid flows out of the pores once the strain relaxes. This leads to type II coalescence. This is only likely if:

1. The liquid content is close to the critical value for a surface layer to appear;

2. There is significant contact area formed during the collision (high St_{def}); and

3. Liquid can move quickly into the contact zone (low viscosity binder and large granule pore size due to large primary particles).

These conditions correspond to a weak, nearly saturated deformable granule. Clearly, type I coalescence is impossible for surface-dry granules. For type II coalescence, the derivation is very similar to that described in Eqs. 6 to 31, except that there is no approach stage ($u_1 = u_0$) and during rebound the liquid layer is only present between the two flattened surfaces (Figure 6). Thus, Eq. 29 becomes

$$\left(\frac{Y_d}{E^*}\right)^{1/2}(St_{def})^{-9/8} < \frac{0.172}{St_{vis}}\left(\frac{\tilde{D}}{h_0}\right)^2\left(\frac{h_0^2}{h_a^2}-1\right)$$

$$\left[1-7.36\left(\frac{Y_d}{E^*}\right)(St_{def})^{-1/4}\right]^2. \quad (29a)$$

The permanent deformation δ'' in Eq. 29a is also different from Eq. 18:

$$\delta'' = \left(\frac{8}{3\pi}\right)^{1/2}(St_{def})^{1/2}\tilde{D}\left[1-7.36\left(\frac{Y_d}{E^*}\right)(St_{def})^{-1/4}\right]. \quad (18a)$$

Figure 7 shows the coalescence predictions of Eq. 29a for two cases: h_0 constant and $h_0 = \delta''$. In both cases, the shape of the plot is similar. The curves asymptotically approach a
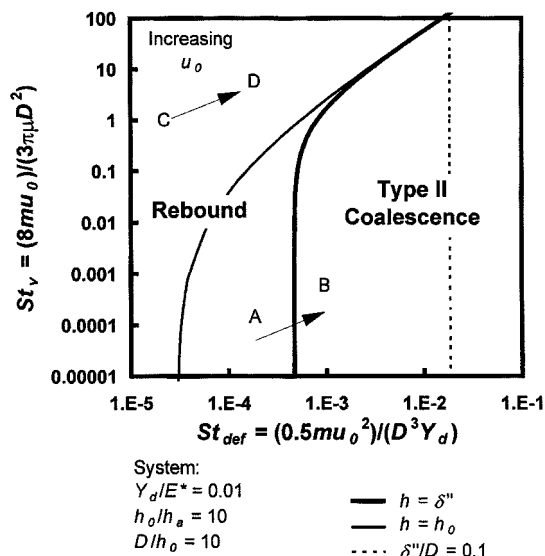
Figure 7. St_v vs. St_{def} showing model predictions for coalescence of surface dry granules.

Table 1. Measured Granule Properties by Iveson and Litster (1998a,b) and Calculated Dimensionless Group ($\rho_g = 1,800$ kg/m^3)

Binder Type	Particle Size (μm)	Binder Content (w/w)	Granule Y_d (kPa)	St_v	St_{def}
Water	19	0.18	31	1482	0.0133
($\mu = 0.0011$	19	0.19	41	1494	0.010
Pa·s)	19	0.21	33	1519	0.013
	31	0.18	70	1482	0.0058
	31	0.19	61	1494	0.0068
	31	0.2	70	1507	0.0059
Glycerol	19	0.214	320	1.39	0.0013
($\mu = 1.1$	19	0.233	370	1.41	0.0012
Pa·s)	19	0.239	450	1.41	0.0010

critical value of St_{def}. For all collisions where St_{def} is below this critical value, coalescence does not occur, regardless of St_v. This critical value occurs when there is no permanent plastic deformation, since there is then no liquid layer during rebound (in Figure 7 the critical value of St_{def} is 1.22×10^{-5} found by setting $\delta'' = 0$ in Eq. 18a). For St_{def} above this critical value, St_v becomes significant, since it indicates the liquid viscosity.

Comparing the two different assumptions about h_0, assuming a constant value of h_0 gives a greater likelihood of coalescence since there is always a large amount of liquid present, whereas using $h_0 = \delta''$ means that for low deformations, very little liquid is present. Currently, we have no good quantitative estimate for h_0, but expect it will be a function of the extent of granule deformation and the granule saturation (liquid content). The formation of bonds between surface-dry granules during collision is the subject of ongoing research (Iveson and Page, 1998).

Comparison with laboratory granulation data

The coalescence criteria just discussed should help explain observed phenomena in batch granulation data. Iveson et al. (1998a,b) measured the dynamic yield strength and granule growth behavior for glass ballotini granulated with several liquid binders in a laboratory batch granulation drum. Table 1 lists the measured properties and derived dimensionless groups for their system. The Stokes numbers are calculated based on the peripheral drum speed $\omega D_{drum}/2$ which is the maximum collision velocity a granule is likely to experience in the drum (Adetayo et al., 1993). Iveson et al. (1998a) did not measure the elastic modulus of their granules, but static measurements from other workers suggest that Y_d/E is of the order 0.01 to 0.05 for these material (such as Holm et al., 1985). The water and glycerol binders cover viscosities ranging from 0.001 Pa·s to 1 Pa·s.

Figure 8 shows the plot of St_v vs. St_{def} calculated from Eqs. 29 and 34, while Figure 9 shows the growth behavior for

these systems. The two curves give the boundaries for type I and type II coalescence. The dimensionless parameters used in the calculations are listed in Table 2. The weak, water-bound granules grew by steady growth where deformation is generally important (Figure 9a). Most of these points are located in the type II coalescence region, with some points located in the rebound region. For the strong glycerol-bound granules, St_v was much smaller and the systems were on the type I—type II transition boundary. These systems grew by induction growth once liquid was available at the granule surfaces (Figure 9b). Although this result is far from conclusive, it does at least confirm the plausibility of the model.

Comparison of coalescence kernels with granule growth regimes

Iveson and Litster (1998a) proposed a growth regime map for liquid-bound granulation systems. They identified
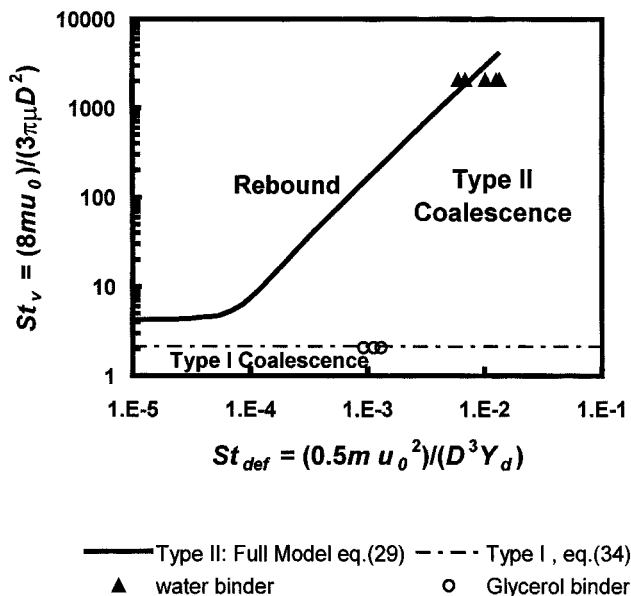

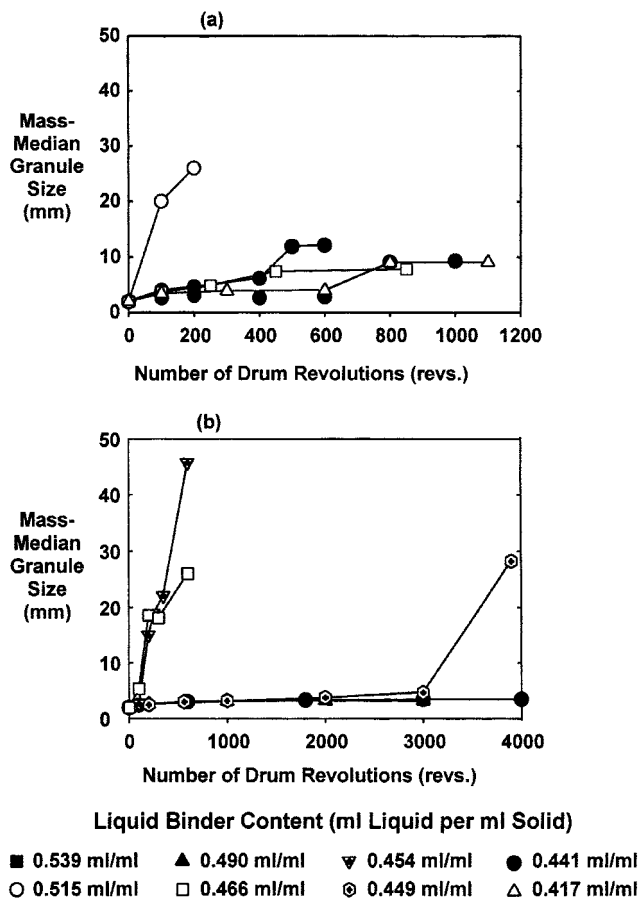Figure 8. Experimental validation of the two coalescence criteria.

Figure 9. Drum granulation growth data for 31-μm ballotini with: (a) water and (b) glycerol binder (Iveson and Litster, 1998a).

Liquid Binder Content (ml Liquid per ml Solid)

■ 0.539 ml/ml   ▲ 0.490 ml/ml   ▽ 0.454 ml/ml   ● 0.441 ml/ml
○ 0.515 ml/ml   □ 0.466 ml/ml   ⊚ 0.449 ml/ml   △ 0.417 ml/ml

three main types of growth: *steady growth* of subsaturated, deformable granules (coarse, narrowly sized particles; low viscosity and surface tension binders; and large granulator impact velocities); *induction growth* of slowly consolidating, nondeformable granules (fine, widely sized powders; high viscosity and surface tension binders; and low-impact velocities); and *rapid growth* of oversaturated, deformable granules (high binder contents).

Comparing these growth regimes with the existing coalescence models (Table 3), we note that the model of Ennis et al. (1991), which assumes elastic spheres with surface liquid layers, applies to induction growth systems once they have consolidated sufficiently to squeeze liquid binder to the surface. Rapid-growth systems are described by the current

Table 2. Parameters Used in the Validation of Coalescence Criteria

Parameters	Value
D/D_p	158 (3/0.019)[†]
Y_d/E^*	0.008
k	0.5
$\nu - \epsilon s^*$	0.2 * 0.4

[†]To Simplifying the calculations, a D_p value of 19 μm was used for all cases.

Table 3. Different Growth Regimes with the Existing Coalescence Models

Growth Regime	Granule Properties	Surface Liquid	Model
Induction	Elastic	Yes	Ennis et al. (1991), Eq. 23
Steady Growth	Elastic– Plastic	Post collision only	Current model with surface dry extension, Eq. 29a
Rapid Growth	Elastic– Plastic	Yes	Current model, Eq. 29

model, which assumes granules are both deformable and surface wet. The extension of the model to include surface-dry granules applies to steady growth systems. Hence, there now exist fundamentally derived coalescence kernels that can be used to quantitatively describe all the major types of granule growth identified in the literature. (Note, however, that the model for surface-dry granules will need to be developed further through a better understanding of how bonds are formed between colliding granules, both due to interparticle attractions and liquid binder being squeezed into the bond zone.)

Conclusions

A model for predicting the coalescence of deformable, surface-wet granules has been developed. This model is an extension of the model of Ennis et al. (1991) to include granule deformation during collisions. The model is written in terms of dimensionless groups such as viscous and deformation Stokes numbers and the ratio of (Y_d/E^*). These variables are bulk parameters of the powder–binder mixture and also functions of the process intensity. The model gives the conditions for two types of coalescence: type I and type II. For type I coalescence, granules coalesce by viscous dissipation in the surface liquid layer before the granule surfaces contact. In type II coalescence, granules surfaces contact and deform. Relative granule velocity is reduced to zero by viscous forces during rebound. Both deformable and nondeformable granules can grow by either mechanism, although deformable granules can coalesce by the type II mechanism over a greater range of St_v. Preliminary validation of the coalescence criterion with drum granulation data is quite encouraging. More work on different powder–binder mixtures is required to confirm the coalescence criterion.

The coalescence criterion developed here has the potential to aid in process and formulation design because it predicts the coalescence behavior of a formulation without the need for extensive laboratory granulation experiments. It can also potentially be used in a population balance model to predict the evolution of granule size distribution during granulation.

Notation

D_p = particle diameter, m
E^* = granule Young's modulus, Pa
e = coefficient of restitution
H = half distance between colliding granules, m

k = proportional constant
r = radial distance from the axis of symmetry in Figure 3d, m
R = granule radius, m
ϵ_0 = initial granule porosity
μ = binder viscosity, Pa·s
ρ_g = granule density, kg/m^3
ρ_s = particle density, kg/m^3
ρ_l = binder density, kg/m^3
ν = Poisson's ratio

Literature Cited

Adams, M. J., and B. Edmondson, "Forces Between Particles in Continuous and Discrete Liquid Media," *Tribology in Particulate Technology*, B. J. Briscoe and M. J. Adams, eds., IOP Publishing Ltd (1987).

Adetayo, A. A., J. D. Litster, and M. Desai, "The Effect of Process Parameters on Drum Granulation of Fertilizers with Broad Size Distributions," *Chem. Eng. Sci.*, **48**, 3951 (1993).

Davis, R. H., J. Serayssol, and E. J. Hinch, "The Elastohydrodynamic Collision of Two Spheres," *J. Fluid Mech.*, **163**, 479 (1986).

Ennis, B. J., G. Tardos, and R. Pfeffer, "A Micro-Level Based Characterisation of Granulation Phenomena," *Powder Technol.*, **65**, 257 (1991).

Ennis, B. J., and J. D. Litster, "Particle Size Enlargement," *Perry's Chemical Engineers' Handbook*, R. Perry and D. Green, eds., Mc-Graw-Hill, New York (1997).

Franks, G. V., and F. F. Lange, "Plastic Flow of Saturated Alumina Powder Compacts: Pair Potential and Strain Rate," *AIChE J.*, **45**, 1830 (1999).

Holm, P., T. Schaefer, and H. G. Kristensen, "Granulation in High Shear Mixers: V. Power Consumption and Temperature Changes During Granulation," *Powder Technol.*, **43**, 213 (1985).

Hoornaert, F., P. A. L. Wauters, G. M. H. Meesters, S. E. Pratsinis, and B. Scarlett, "Agglomeration Behaviour of Powders in a Lödige Mixer Granulator," *Powder Technol.*, **96**, 116 (1998).

Iveson, S. M., and J. D. Litster, "Granule Growth Regime Map for Liquid-Bound Granules," *AIChE J.*, **44**, 1510 (1998a).

Iveson, S. M., and J. D. Litster, "Liquid-Bound Granule Impact Deformation and Coefficient of Restitution," *Powder Technol.*, **99**, 234 (1998b).

Iveson, S. M., and N. W. Page, "Bond Strength Formed Between Liquid-Bound Pellets During Compression," *CHEMECA '98*, Port Douglas, Queensland, Australia (1998).

Johnson, K. L., *Contact Mechanics*, Cambridge Univ. Press, New York (1987).

Kapur, P. C., "Balling and Granulation," *Adv. Chem. Eng.*, **10**, 55 (1978).

Kristensen, H. G., P. Holm, and T. Schaefer, "Mechanical Properties of Moist Agglomerates in Relation to Granulation:" *Powder Technol.*, **44**, 227 (1985).

Larsson, R., and E. Höglund, "Elastohydrodynamic Lubrication at Impact Loading," *Trans. ASME*, **116**, 770 (1994).

Lian, G., M. J. Adams, and C. Thornton, "Elastohydrodynamic Collisions of Solid Spheres," *J. Fluid Mech.*, **311**, 141 (1996).

Moseley, J. L., and T. J. O'Brien, "A Model for Agglomeration in a Fluidised Bed," *Chem. Eng. Sci.*, **48**, 3043 (1993).

Ouchiyama, N., and T. Tanaka, "The Probability of Coalescence in Granulation Kinetics," *Ind. Eng. Chem. Process Des. Dev.*, **14**, 286 (1975).

Schaefer, T., P. Holm, and H. G. Kristensen, "Wet Granulation in a Laboratory Scale Shear Mixer," *Pharm. Ind.*, **52**, 1147 (1990).

Simons, S. J. R., J. P. K. Seville, and M. J. Adams, "Mechanisms of Agglomeration," *Int. Symp. Agglomeration*, Nagoya, Japan (1993).

Tardos, G. I., M. I. Khan, and P. R. Mort, "Critical Parameters and Limiting Conditions in Binder Granulation of Fine Powders," *Powder Technol.*, **94**, 245 (1997).

Thornton, C., and Z. Ning, "A Theoretical Model for the Stick/Bounce Behavior of Adhesive, Elastic-Plastic Spheres," *Powder Technol.*, **99**, 154–162 (1998).